

Electronic Supplementary Information

Influencing Prototropy by Metal Ion Coordination: Supramolecular Transformation of a Dynamer into a Zn-based Toroidal Species

Miroslava Čonková^{a,b}, Wojciech Drożdż^{a,b}, Zygmunt Miłośz^c, Piotr Cecot^{a,b}, Jack Harrowfield^d, Mikołaj Lewandowski^c, Artur R. Stefankiewicz^{a,b*}

^aFaculty of Chemistry
Adam Mickiewicz University
Uniwersytetu Poznańskiego 8, 61-614 Poznań, Poland

^bCenter for Advanced Technologies
Adam Mickiewicz University
Uniwersytetu Poznańskiego 10, 61-614 Poznań

^cNanoBioMedical Centre
Adam Mickiewicz University
Wszechnicy Piastowskiej 3, 61-614 Poznań, Poland

^dInstitut de Science et d'Ingénierie Supramoléculaires (ISIS)
Université de Strasbourg
8 allée Gaspard Monge, 67083 Strasbourg, France

*Corresponding author. E-mail: ars@amu.edu.pl (Artur R. Stefankiewicz)

Table of contents

I. EXPERIMENTAL SECTION.....	4
General methods	4
Figure S1.....	5
Figure S2.....	5
Figure S3.....	6
Figure S4.....	6
Figure S5.....	7
Figure S6.....	7
Synthesis of complex $[\text{Zn}(\text{H}_2\text{L}')_2]$	7
Figure S7.....	8
Figure S8.....	9
Figure S9.....	10
Figure S10.....	10
Figure S11.....	11
Figure S12.....	11
Figure S13.....	12
Figure S14.....	13
Figure S15.....	14
Figure S16.....	15
Figure S17.....	16
Figure S18.....	17
Figure S19.....	18
Figure S20.....	19
Figure S21.....	20
II. MOLECULAR MODELLING	21
Table S1.....	21
Figure S22.....	21
Table S2.....	22
H_2L , L^{2-} anion and $[\text{Zn}(\text{H}_2\text{L}')_2](\text{BF}_4)_2$ structure description.....	23
SambVca 2.1 steric hindrance results.....	24
Figure S23.....	24
Table S4.....	24
III. SCANNING TUNNELING MICROSCOPY	24
General methods for STM experiments:	24
Figure S24.....	25
Figure S25.....	25

I. EXPERIMENTAL SECTION

General methods

Chemicals were purchased from commercial suppliers (Sigma-Aldrich and TriMen Chemicals) and used as received. NMR spectroscopic data were performed on a Bruker UltraShield 300 MHz and 600 MHz spectrometers, calibrated against the residual protonated solvent signal (for ^1H NMR DMSO- d_6 : $\delta = 2.50$, for ^{13}C NMR DMSO- d_6 : $\delta = 39.52$) and are given in ppm. Mass spectra were determined using MALDI-TOF/TOF (Ultrafle extreme, Bruker) spectrometer in DMSO/MeOH mixture. Experiments were performed on DHB (H_2L , Me_2L) and THAP $[\text{Zn}(\text{H}_2\text{L}')_2](\text{BF}_4)_2$ matrix. DSC, TGA and DTG experiments were performed on Simultaneous Thermal Analyzer (STA) 6000, Perkin Elmer. UV/Vis measurements were conducted in solid state on Jasco V-770 spectrophotometer. Fluorescence spectra were made in solid state on Fluorescence Spectrophotometer Hitachi F-7000; light source – 150 W xenon lamp; wavelength speed 240 nm/min. Photographs were made under UV lamp at 254 nm wavelength on digital camera in Samsung S10. Infrared spectra were measured in ATR mode on FT-IR (Nicoletis 50). Both, ligand in amido (H_2L) and iminol ($\text{H}_2\text{L}'$) form were optimized using DFT b3lyp functional and 6-31+G(d,p) basis set. All calculations were carried out using Gaussian 16 rev C.01 software. Steric hindrance of complex $[\text{Zn}(\text{H}_2\text{L}')_2](\text{BF}_4)_2$ was calculated via SambVca 2.1 A web application (<https://www.molnac.unisa.it/OMtools/sambvca2.1/index.html>). The STM measurements were performed using a Bruker Innova Atomic Force Microscope operating in a constant-current STM mode. All the images were recorded using mechanically-cut PtIr tips. Highly-oriented pyrolytic graphite (HOPG) substrate was cleaned using a “Scotch tape” method before each experiment. The use of HOPG was justified by its weak interaction with any adsorbed species which was favouring the formation of molecule-molecule bonds rather than molecule-substrate. The acquired STM images were processed using Gwyddion (gwyddion.net) computer software.

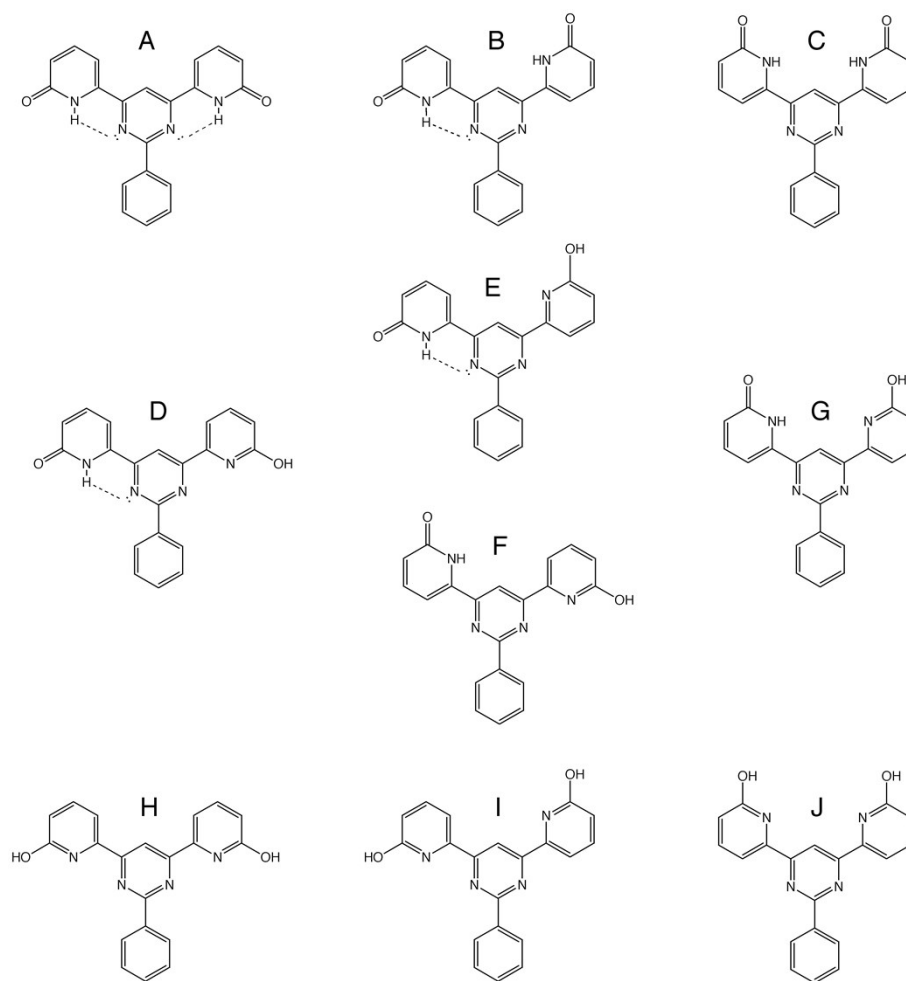


Figure S1. Representations of planar conformations and their tautomeric forms for ligand H_2L . Possible intramolecular H-bonds in certain species are shown as dashed lines. (Nonplanar conformations are also not to be excluded.)

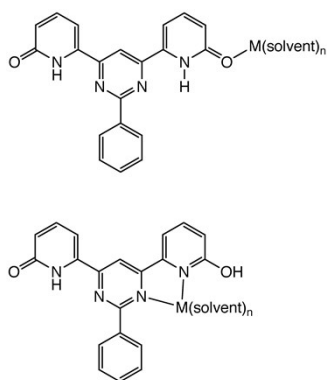


Figure S2. Different possible coordination modes for tautomeric units of ligand H_2L .

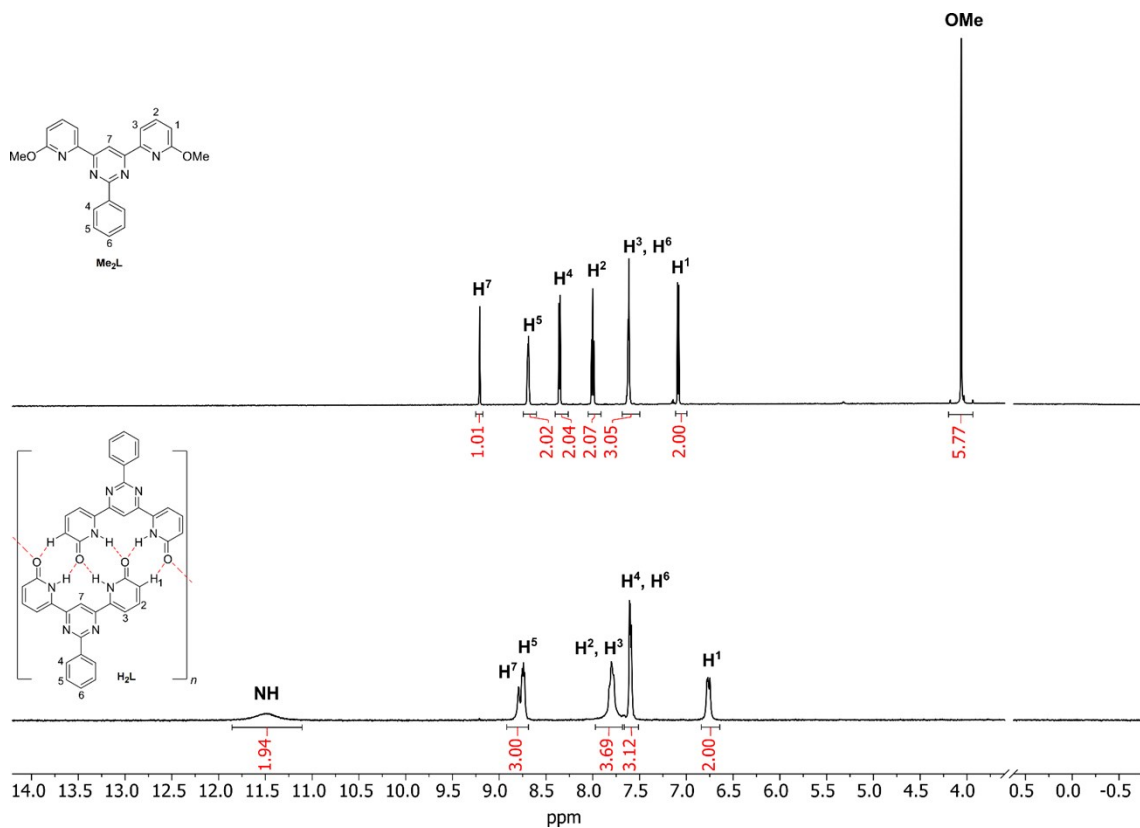


Figure S3. Comparison of ^1H NMR of H_2L dimer and its $-\text{OMe}$ derivative showing broadening of peaks in the lower spectrum, that suggests H-bonds.

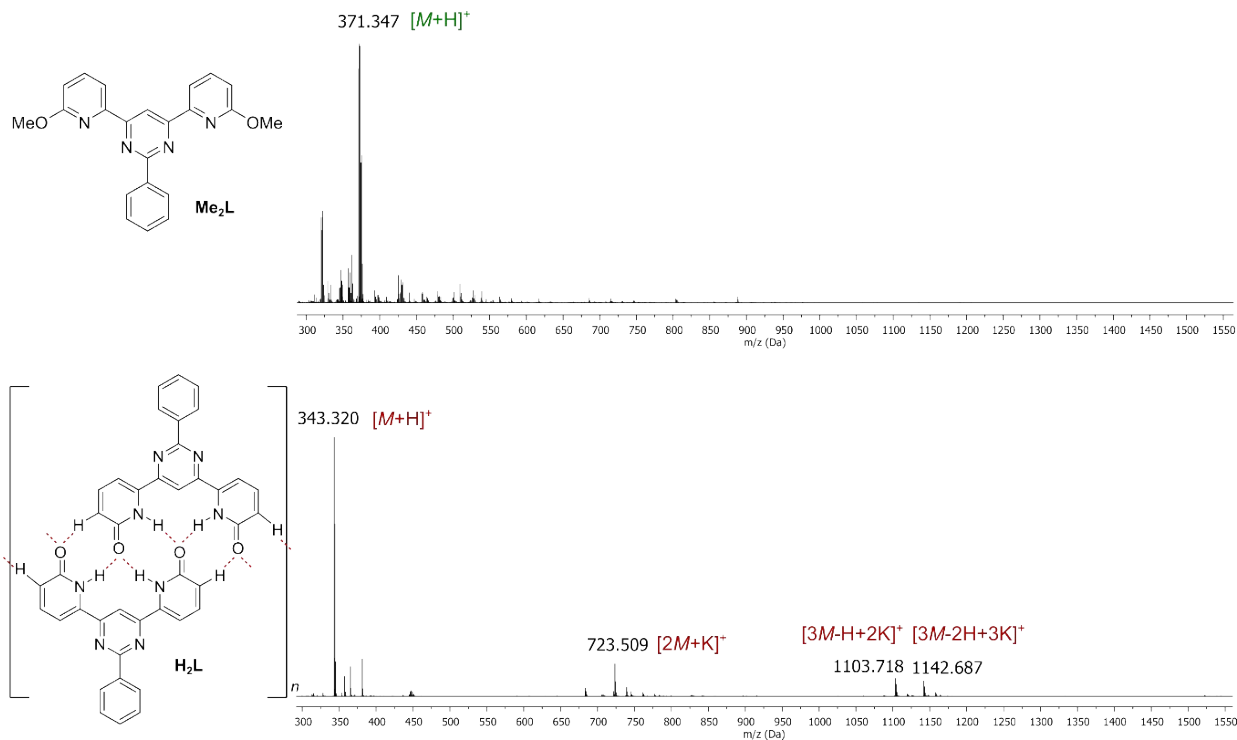


Figure S4. Comparison of MALDI spectra of H_2L and its $-\text{OMe}$ derivative.

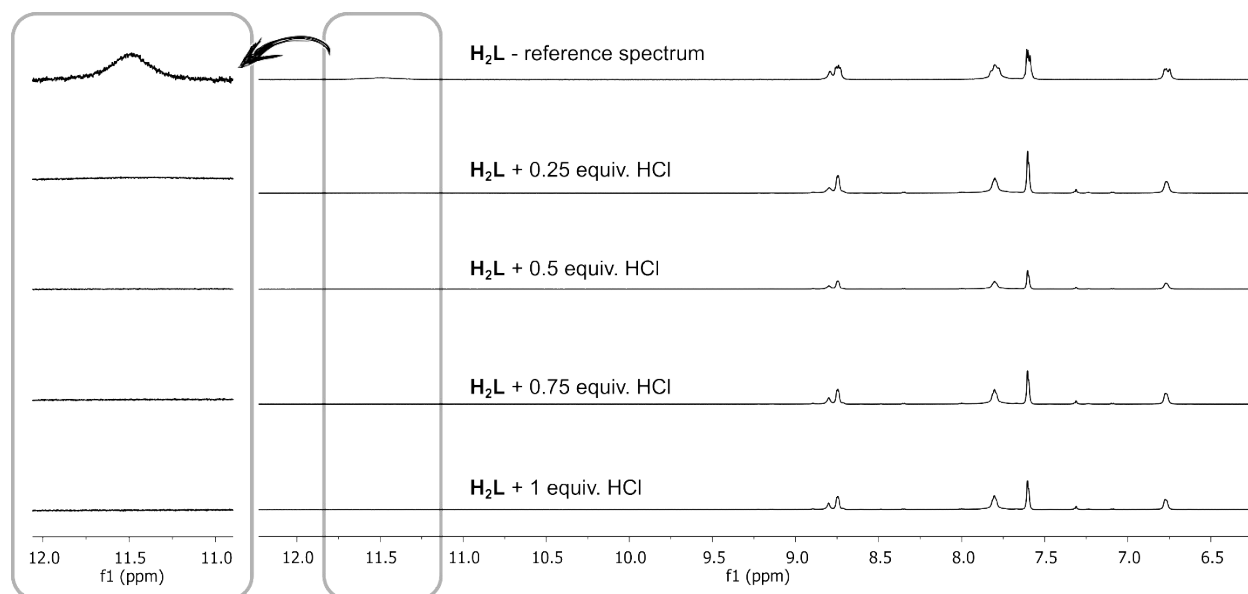


Figure S5. Titration of H_2L with HCl (0.06 M, in DMSO-d_6).

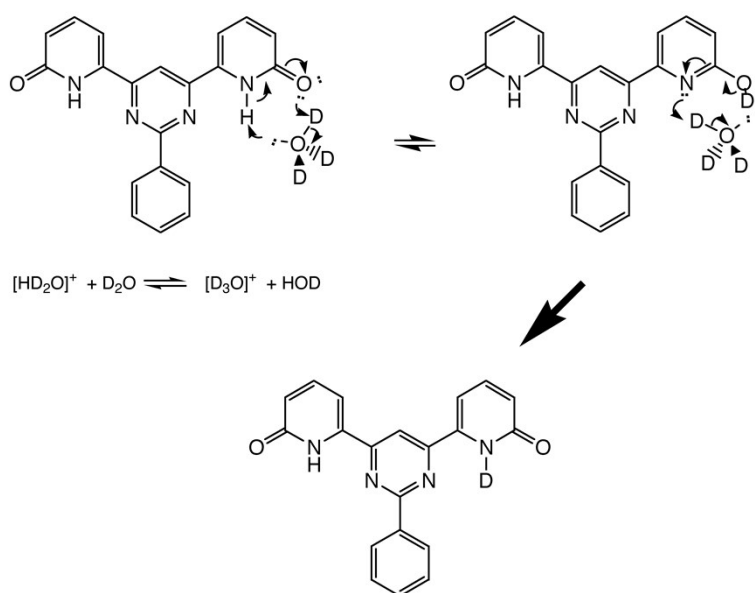


Figure S6. A possible mechanism for acid-catalysed NH exchange in form C of H_2L .

Synthesis of complex $[\text{Zn}(\text{H}_2\text{L}')_2](\text{BF}_4)_2$:

Method A: To the suspension of ligand H_2L (50 mg, 0.15 mmol) in DMSO (10 mL) $\text{Zn}(\text{BF}_4)_2$ (39 mg, 0.15 mmol) was added and the suspension was stirred at 130 °C for 48 h. After the clear solution was cooled to room temperature, methanol and then big portion of diethyl ether was added to precipitate the product. Yellow solid was centrifuged, washed several times with diethyl ether and dried under vacuum.

Method B: To the suspension of ligand H_2L (50 mg, 0.15 mmol) in DMSO (10 mL) NaOH (12 mg, 0.3 mmol) solution in water (1 mL) was added. After stirring at ambient temperature for 0.5 hour $\text{Zn}(\text{BF}_4)_2$ (39 mg, 0.15 mmol) was added and the mixture was stirred at ambient temperature for 24 h. After methanol and big portion of diethyl ether was added to precipitate the product. Yellow solid was centrifuged, washed several times with diethyl ether and dried under vacuum.

^1H NMR (600 MHz, DMSO-d_6) δ 11.76 (bs, 1H), 11.25 (bs, 1H), 8.91–8.60 (m, 3H), 7.91–7.71 (m, 4H), 7.64–7.57 (m, 3H), 6.88–6.63 (m, 2H). ESI-TOF-MS: for $[\text{C}_{40}\text{H}_{27}\text{N}_8\text{O}_4\text{Zn}]^+$ calc. $m/z = 747.1441$, found 747.1419.

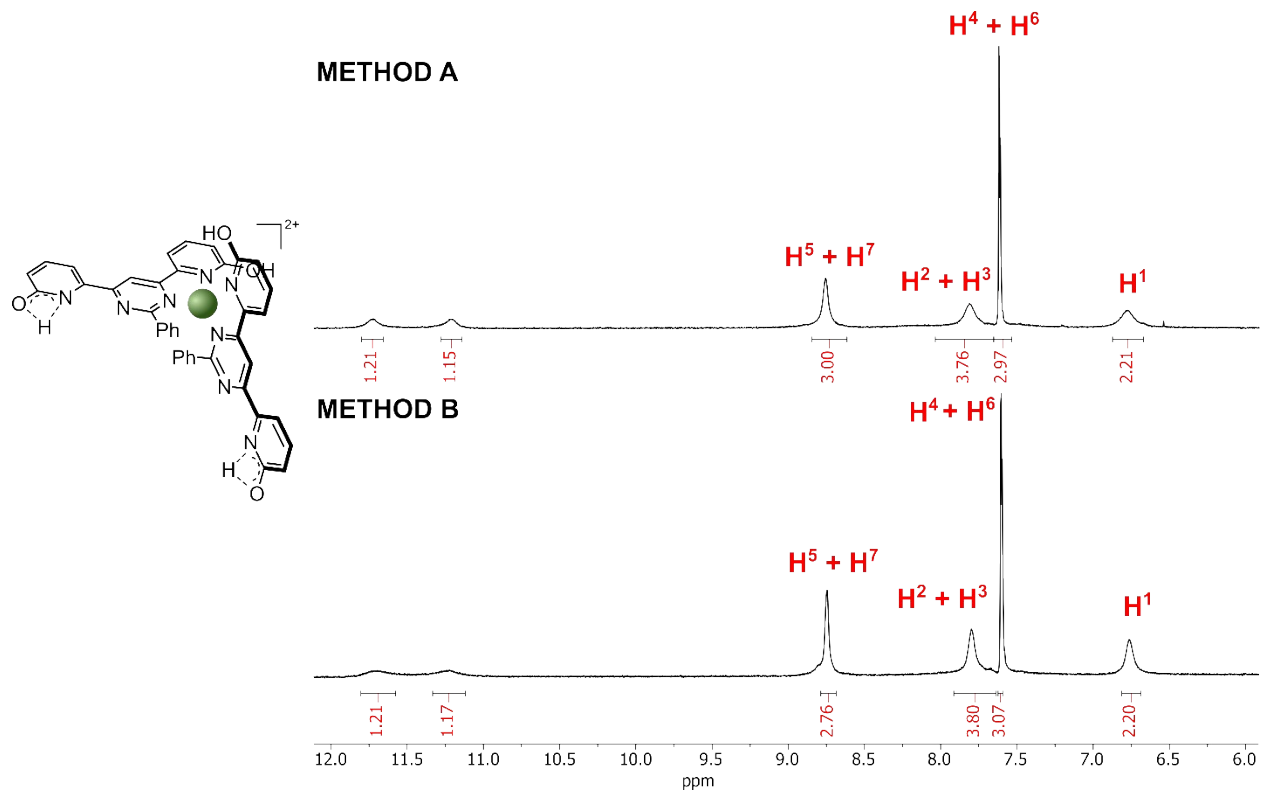


Figure S7 ^1H NMR spectra of $[\text{Zn}(\text{H}_2\text{L}')_2](\text{BF}_4)_2$ prepared by method A and B.

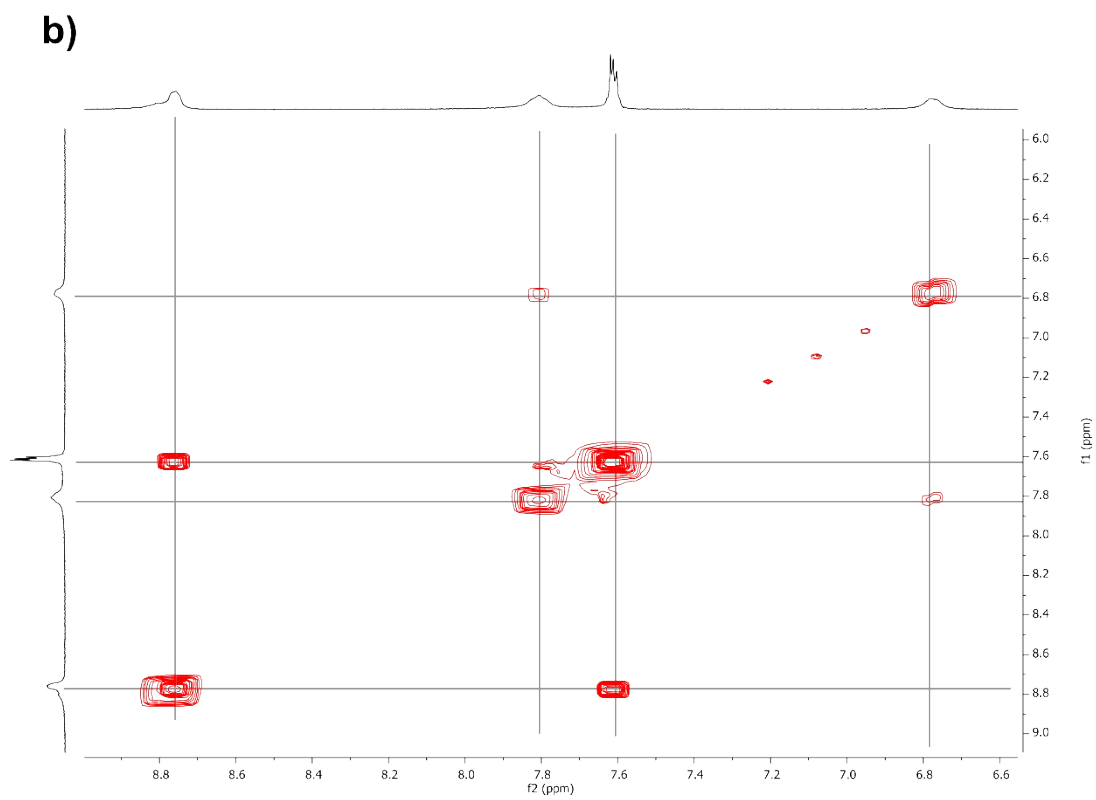
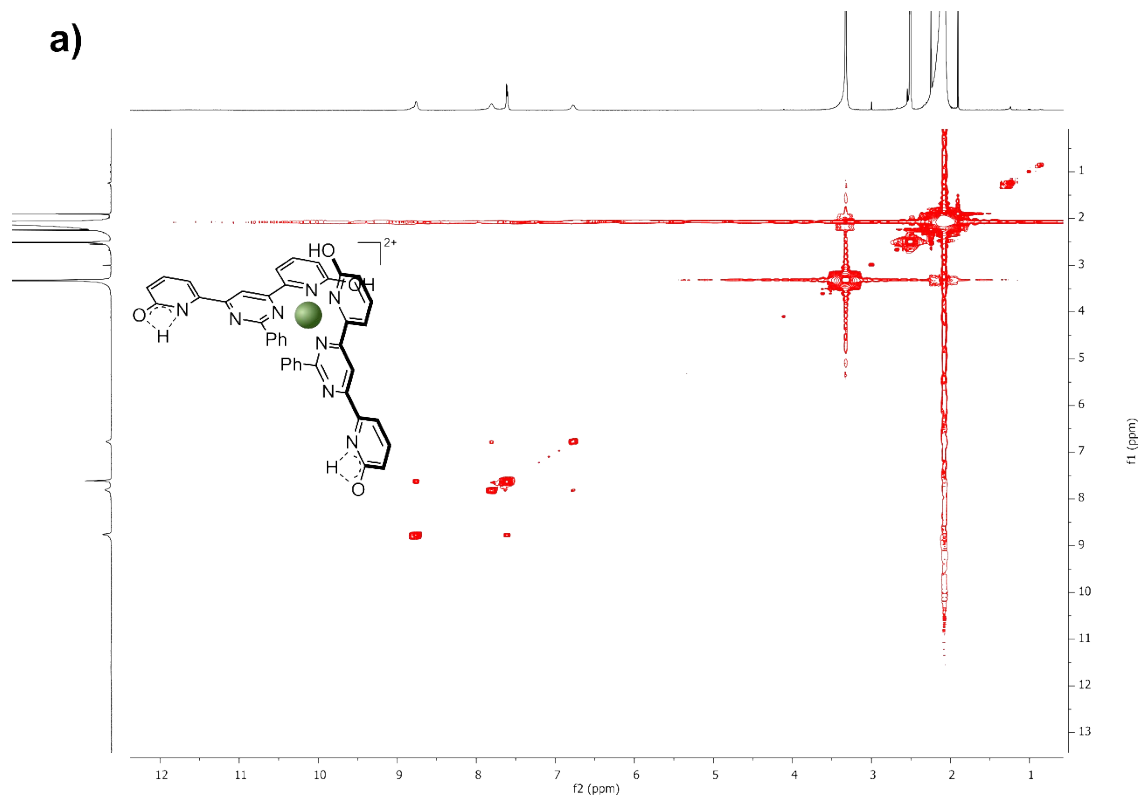


Figure S8. 1H - 1H COSY NMR spectrum of $[Zn(H_2L')_2](BF_4)_2$ (a – whole spectrum, b – part of the spectrum)

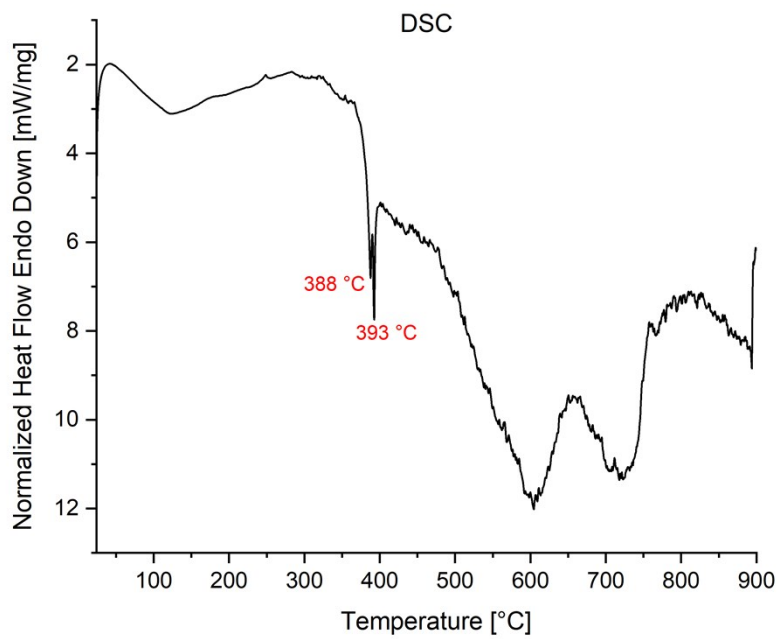


Figure S9. Differential scanning calorimetry analysis of complex [Zn(H₂L')₂](BF₄)₂

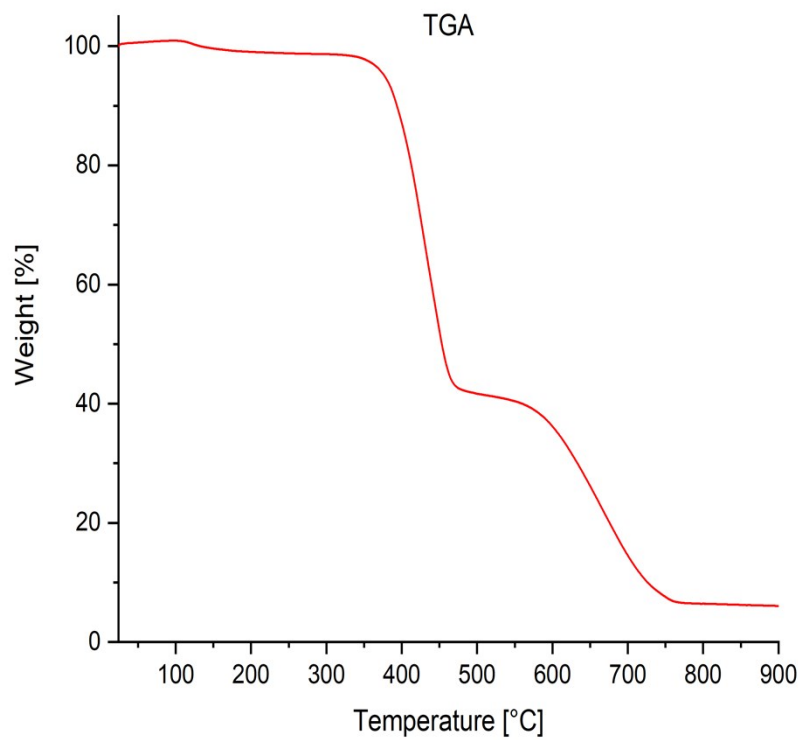


Figure S10. Thermogravimetric analysis of complex [Zn(H₂L')₂](BF₄)₂

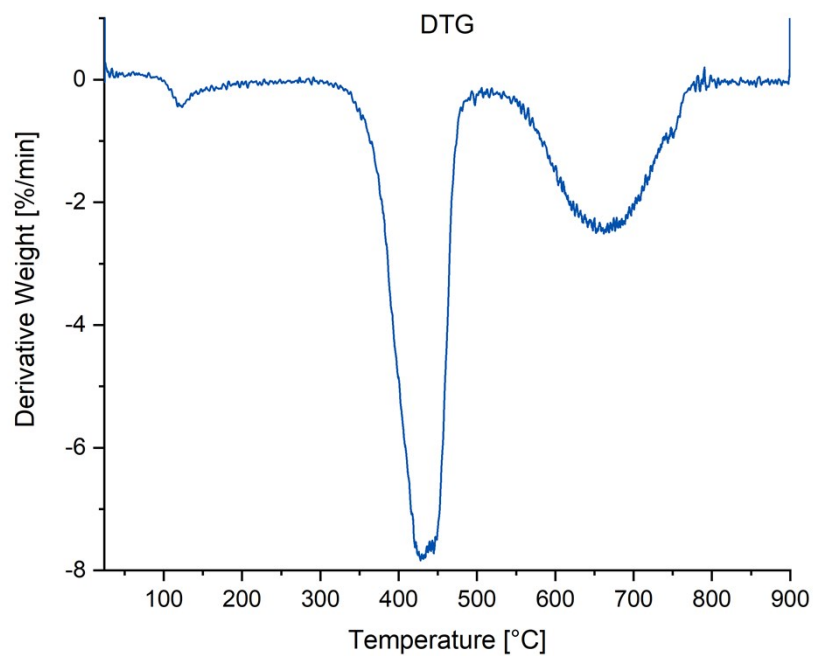


Figure S11. Difference thermogravimetric analysis of complex $[\text{Zn}(\text{H}_2\text{L}')_2](\text{BF}_4)_2$

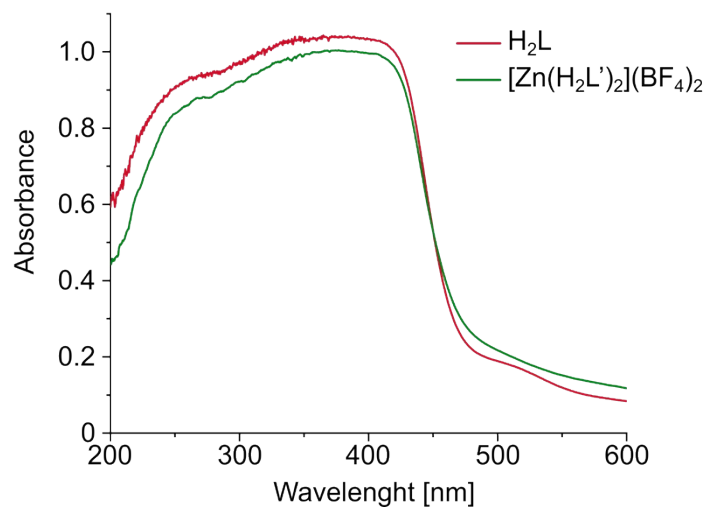


Figure S12. UV-Vis spectra of H_2L and $[\text{Zn}(\text{H}_2\text{L}')_2](\text{BF}_4)_2$ in solid state

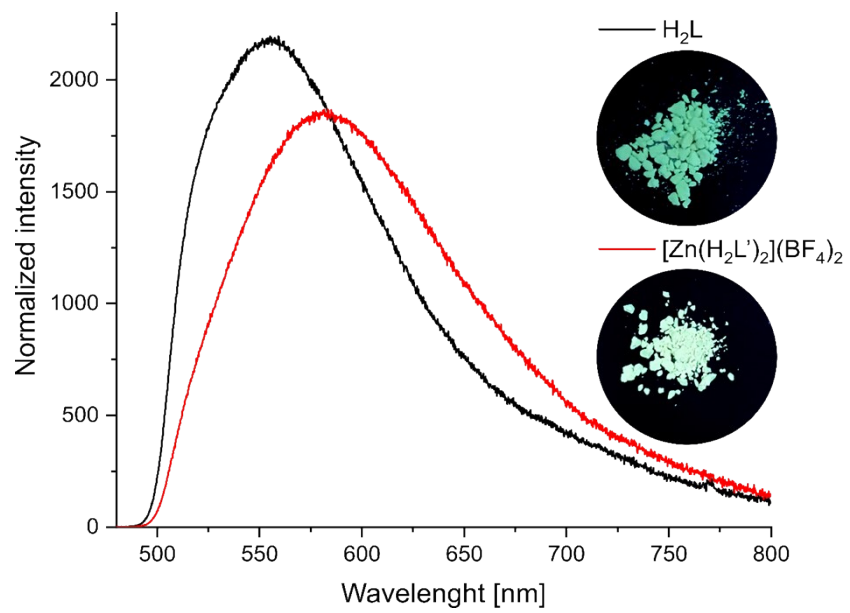


Figure S13. Fluorescence spectra of H_2L and $[Zn(H_2L')_2](BF_4)_2$ in solid state and photographs under UV lamp (254 nm)

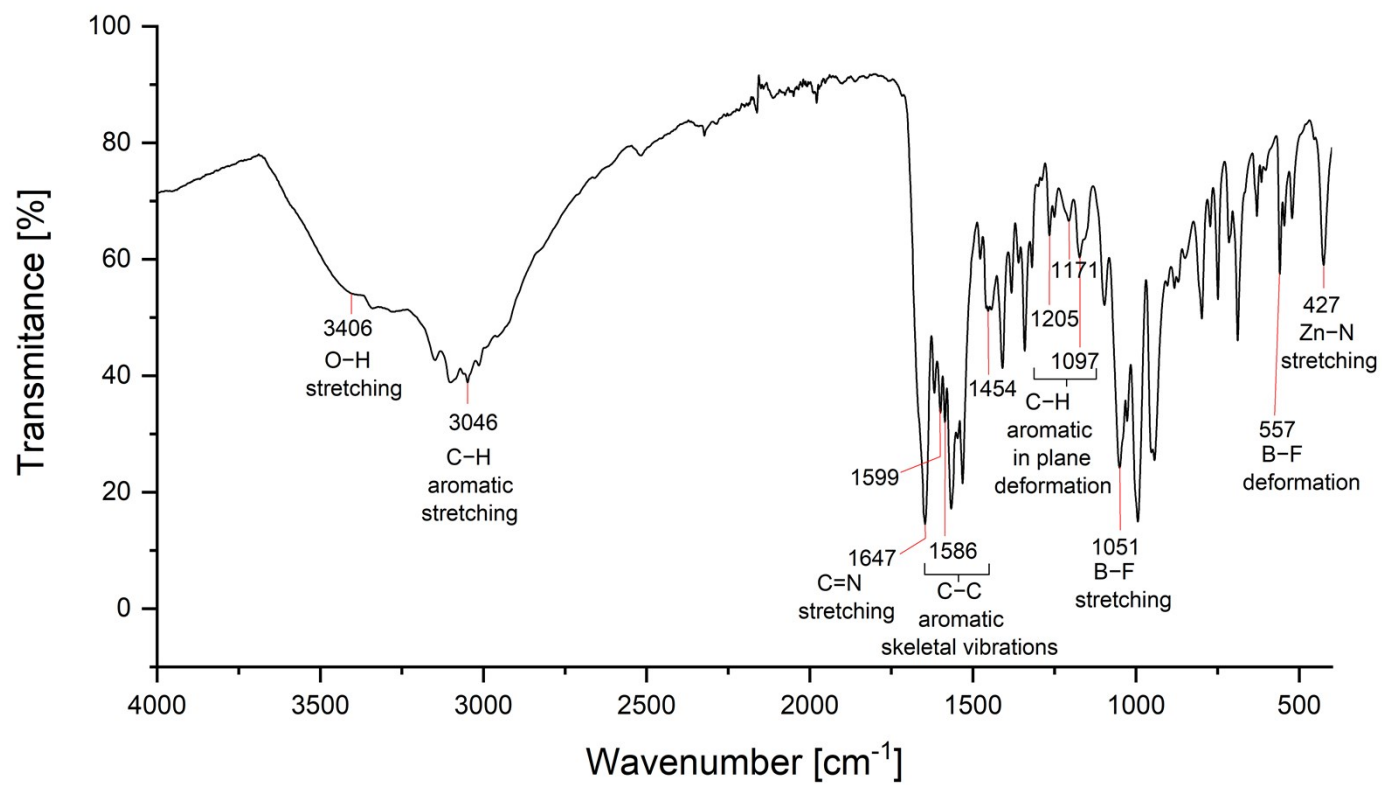


Figure S14. ATR-IR spectrum of complex $[\text{Zn}(\text{H}_2\text{L}')_2](\text{BF}_4)_2$

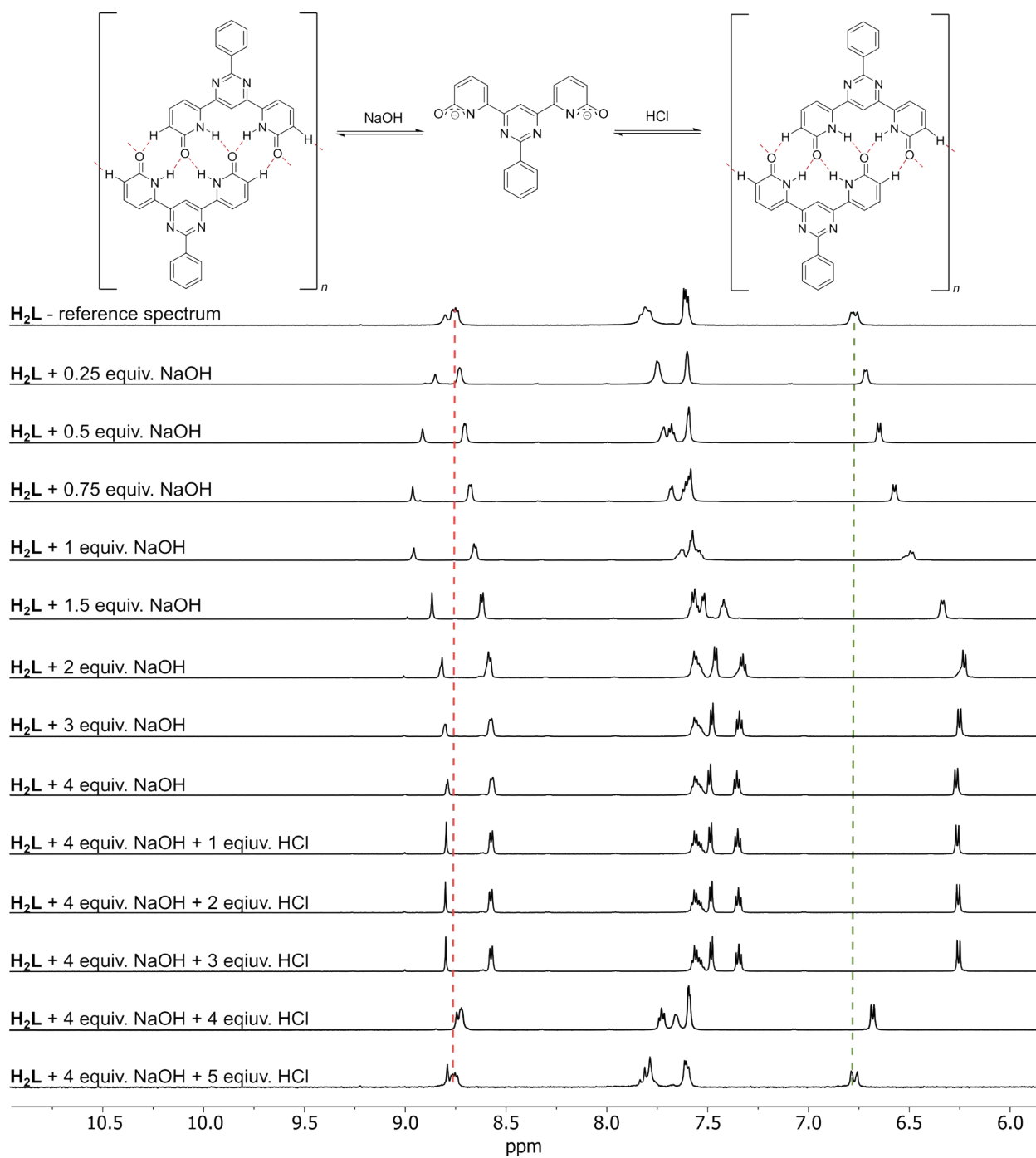


Figure S15. Titration of H_2L with NaOH (0.12 M in $DMSO-d_6/D_2O = 1:1$) causing L^{2-} formation, followed by incremental addition of HCl 0.06 M, in $DMSO-d_6$. NMR spectra were measured right after the addition. Excess of both NaOH and HCl were used to speed up the transformations.

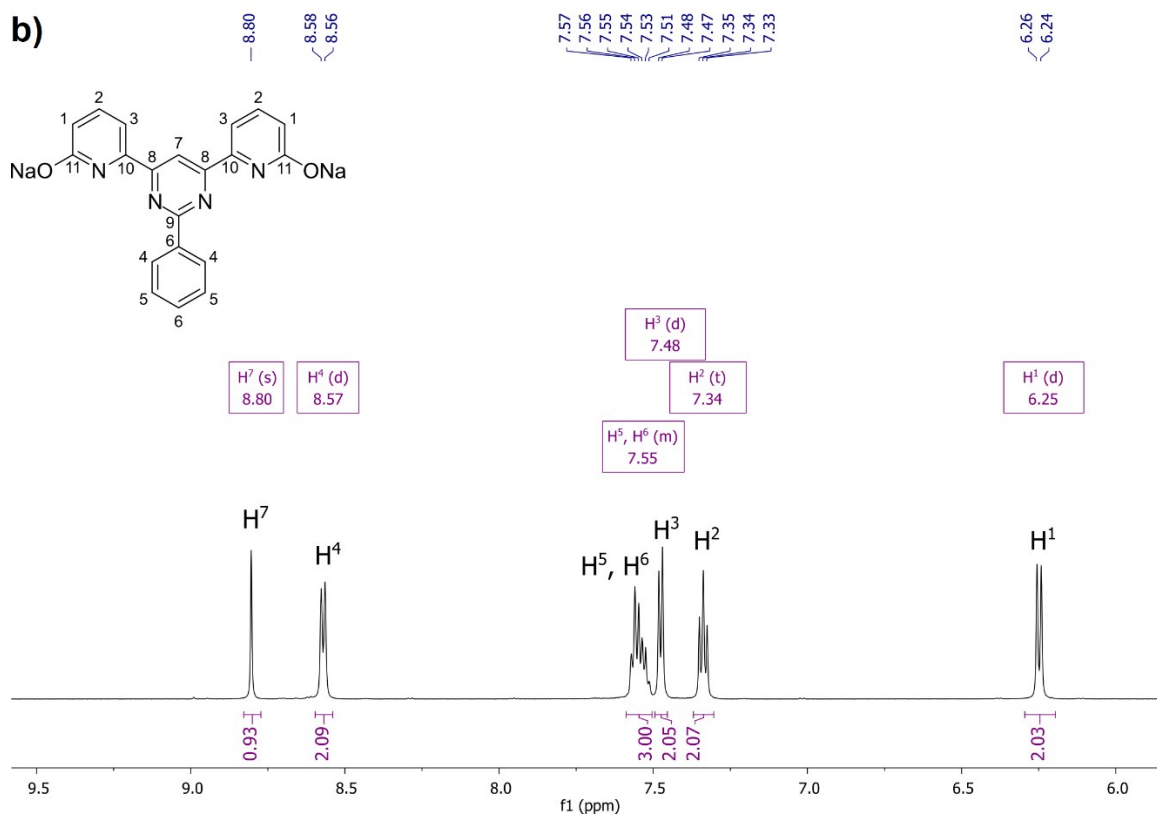
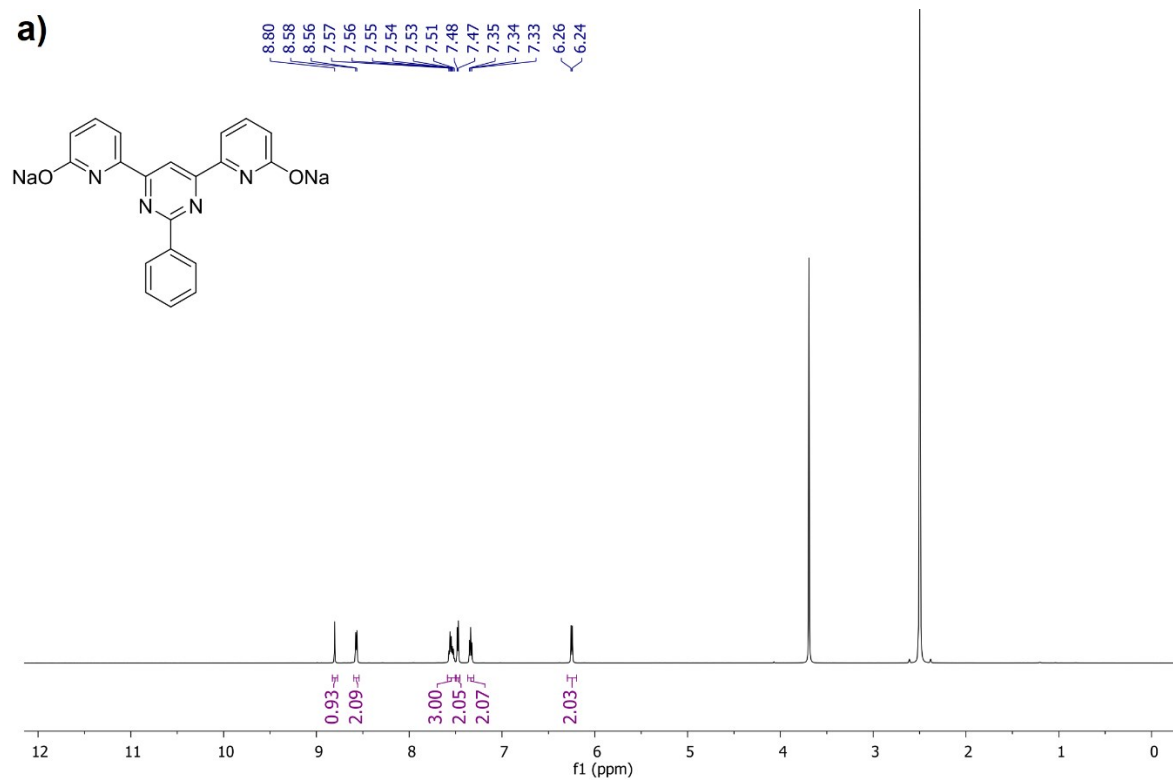


Figure S16. ¹H NMR spectrum of L²- monomer (a – whole spectrum, b – part of the spectrum)

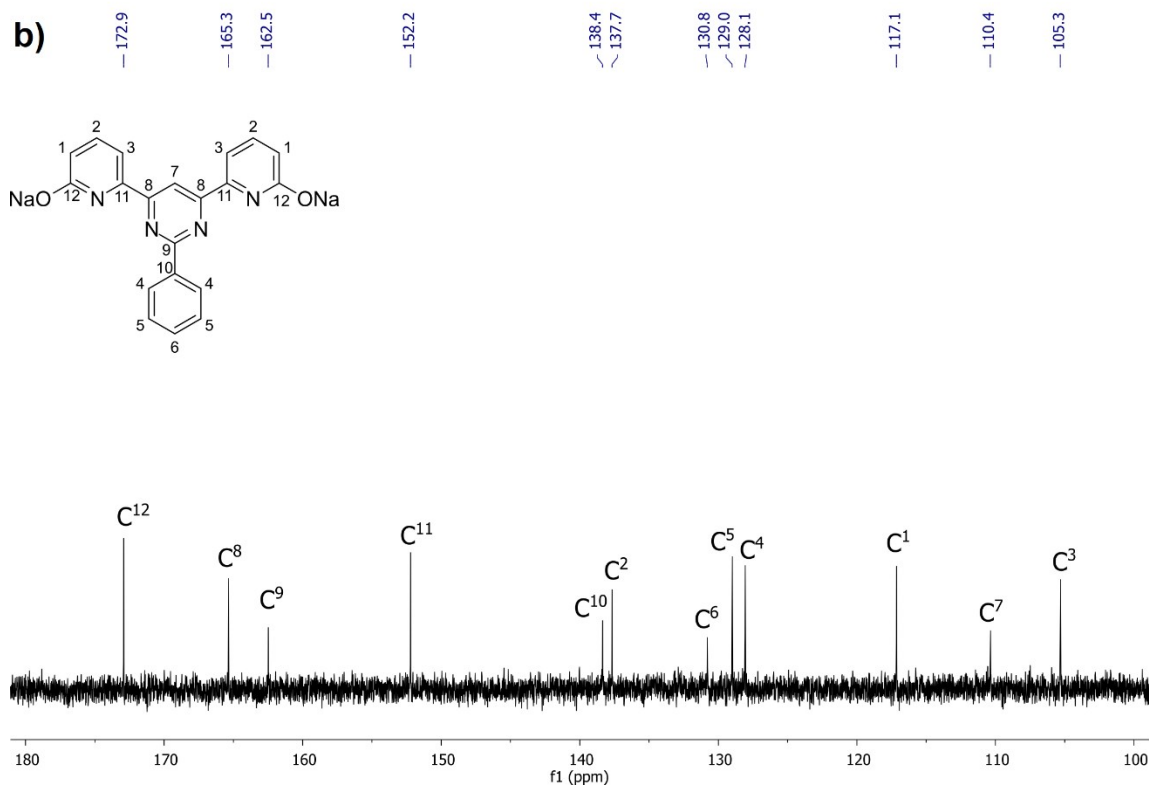
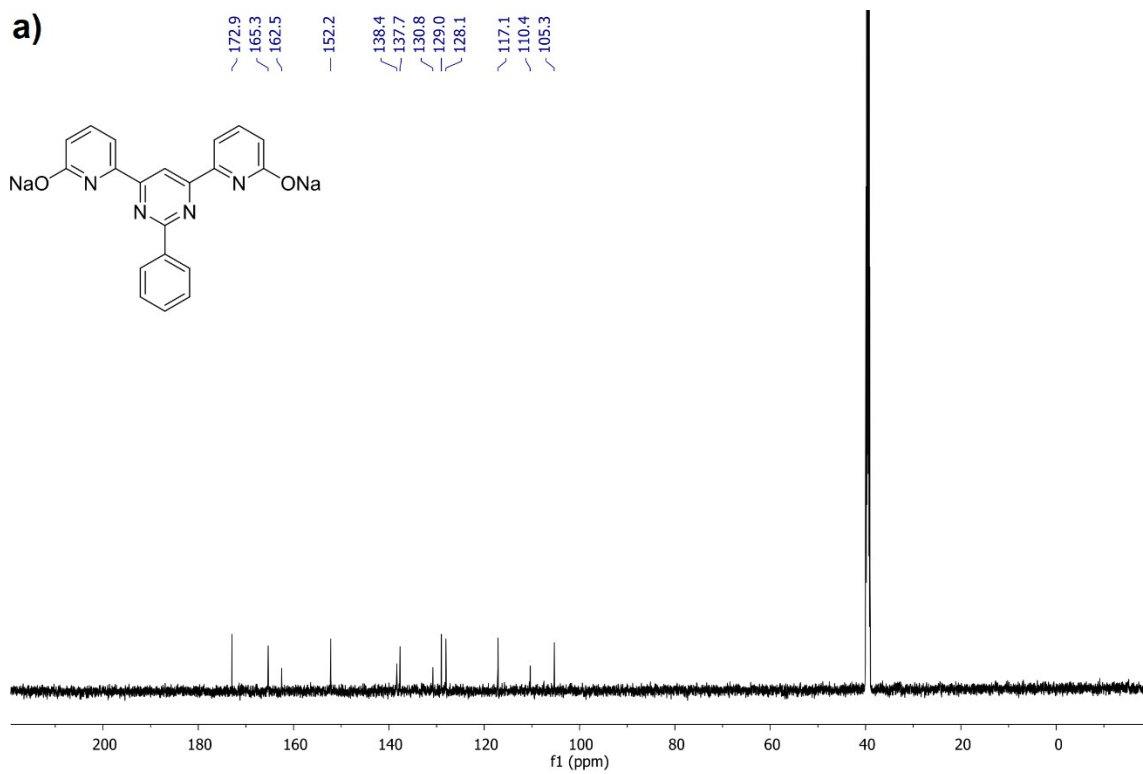


Figure S17. ^{13}C NMR spectrum of L^2 - monomer (a – whole spectrum, b – part of the spectrum)

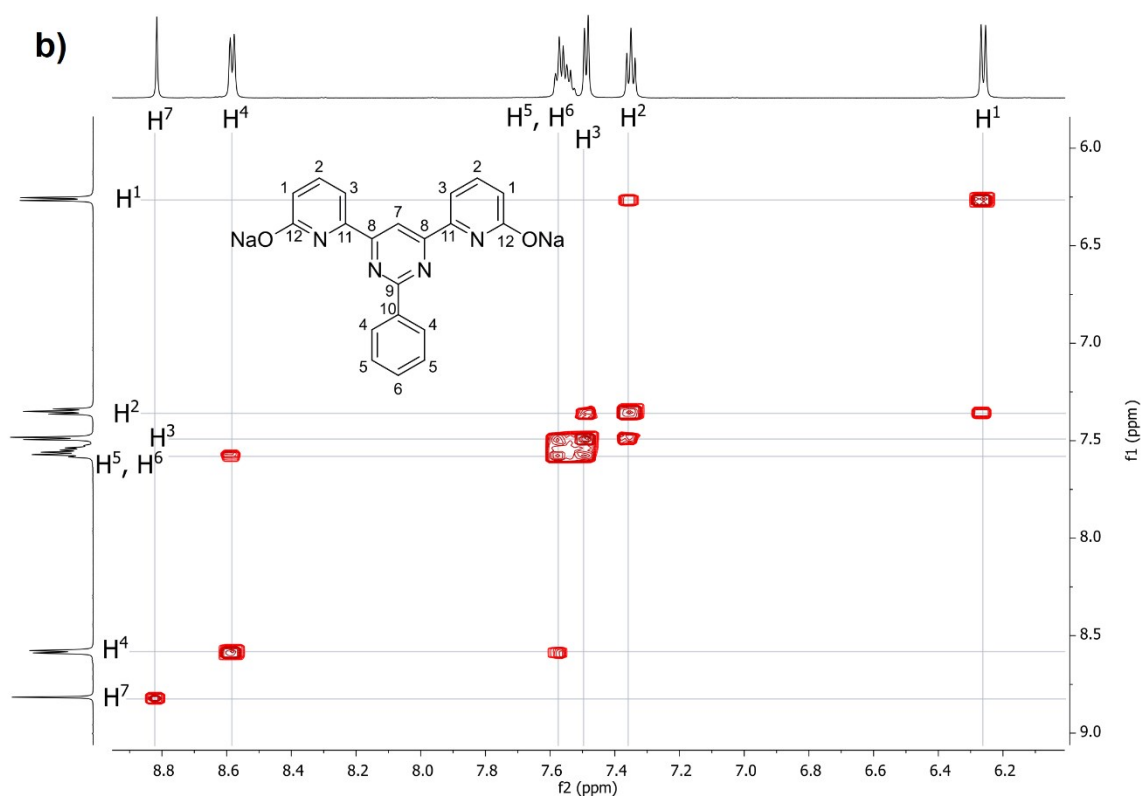
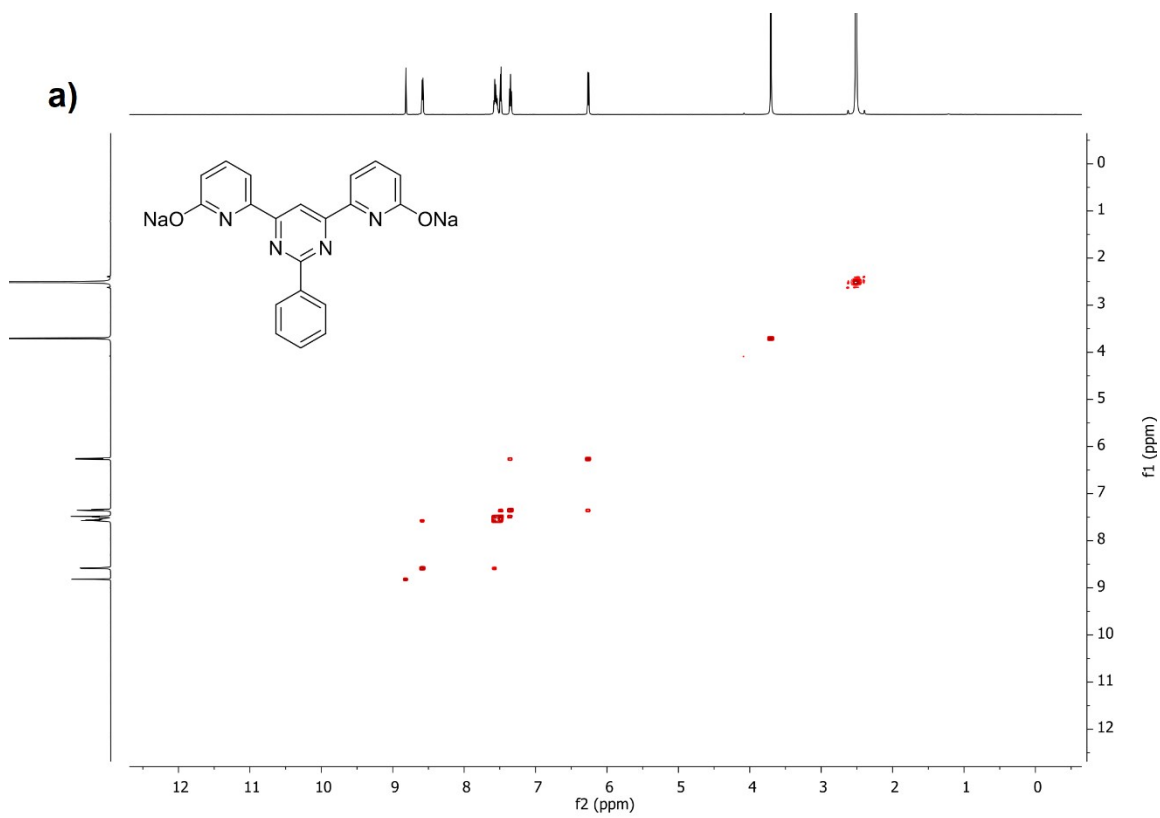
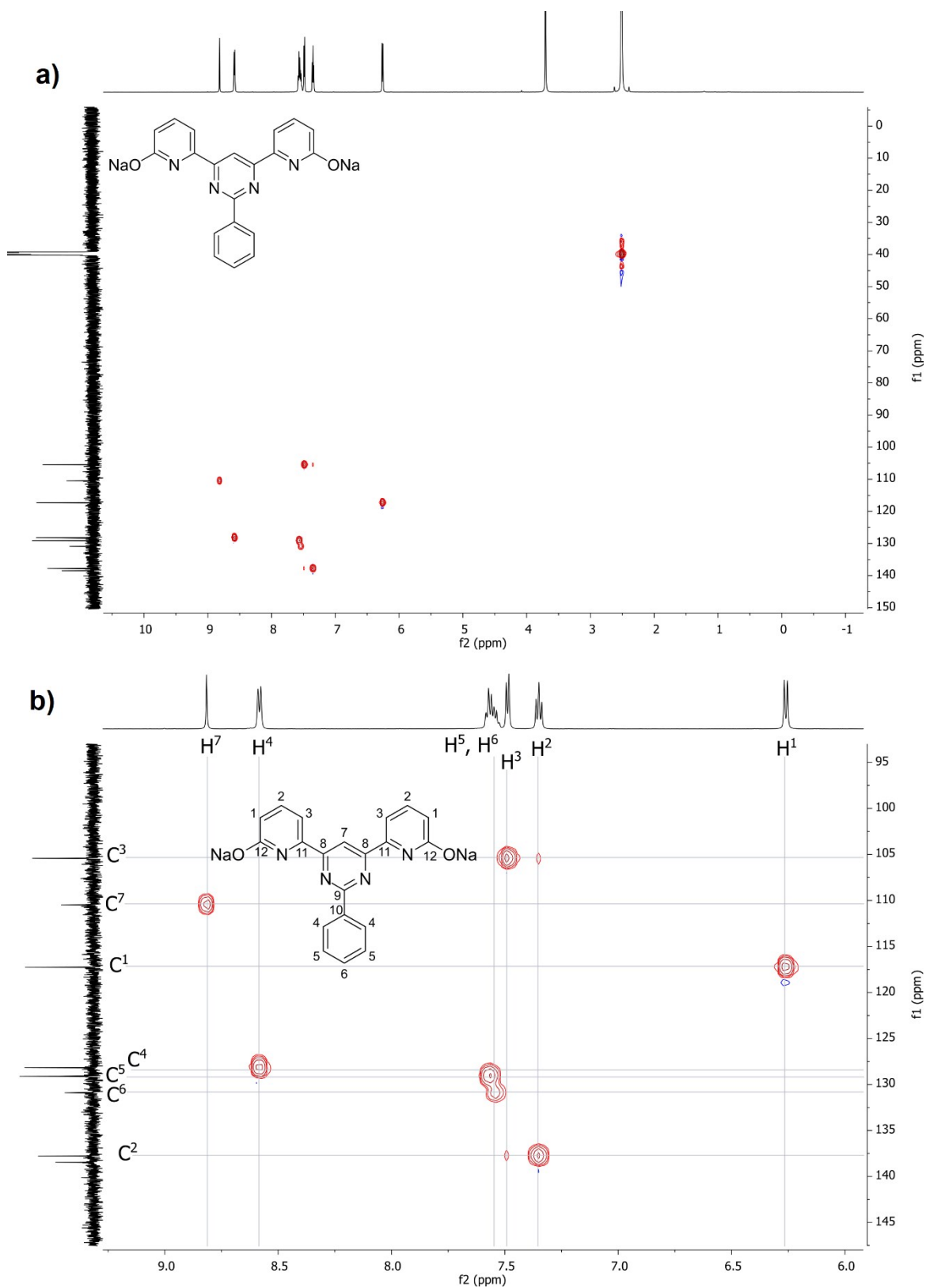


Figure S18. ^1H - ^1H COSY NMR spectrum of L^2- monomer (a – whole spectrum, b – part of the spectrum)



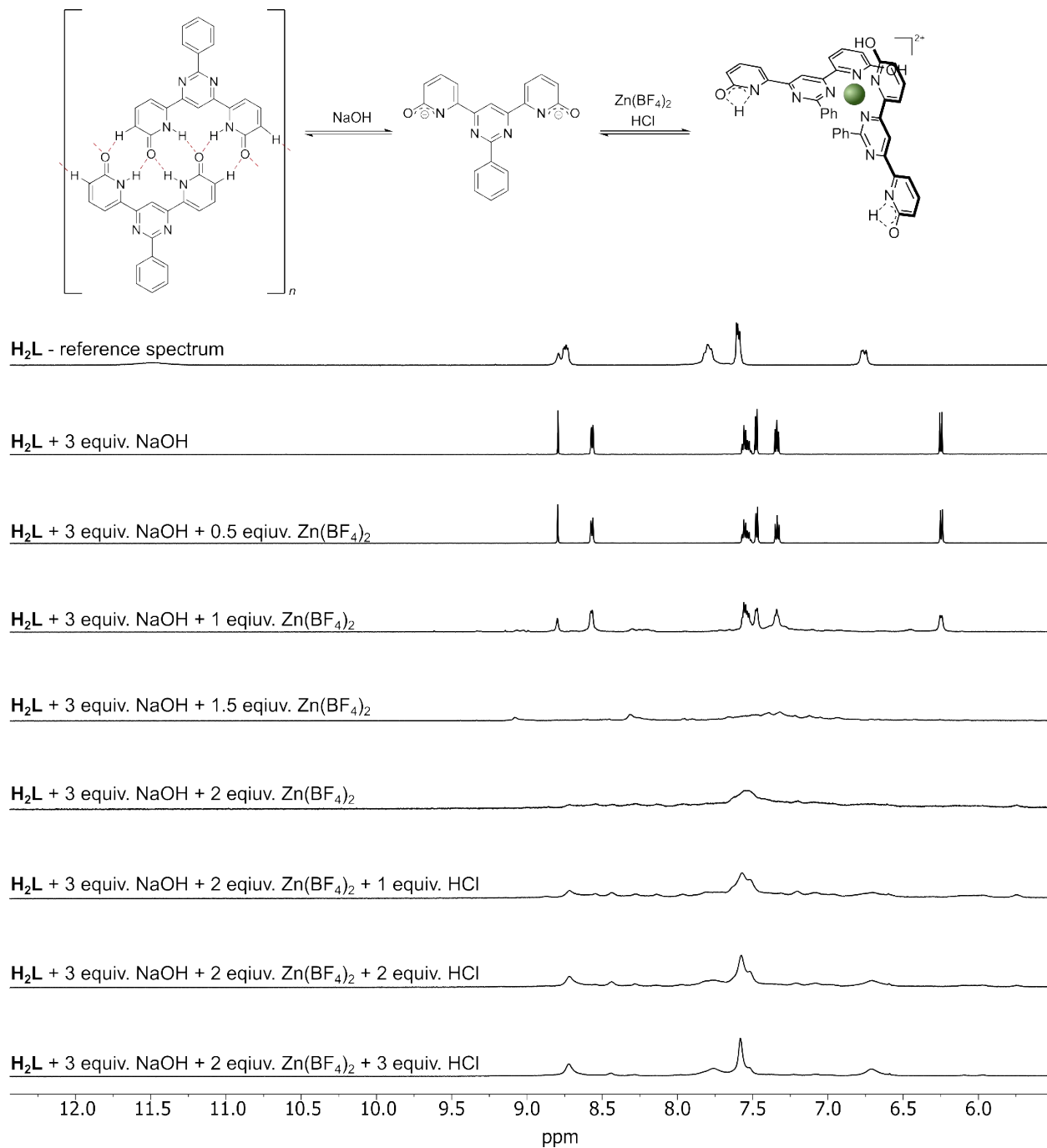


Figure S20. Titration of H_2L with NaOH (0.12 M in $DMSO-d_6/D_2O = 1:1$) causing L^{2-} formation, following by incremental addition of $Zn(BF_4)_2$ (0.12 M in $DMSO-d_6$) and neutralization by HCl (0.06 M, in $DMSO-d_6$) forming $[Zn(H_2L^*)_2](BF_4)_2$.

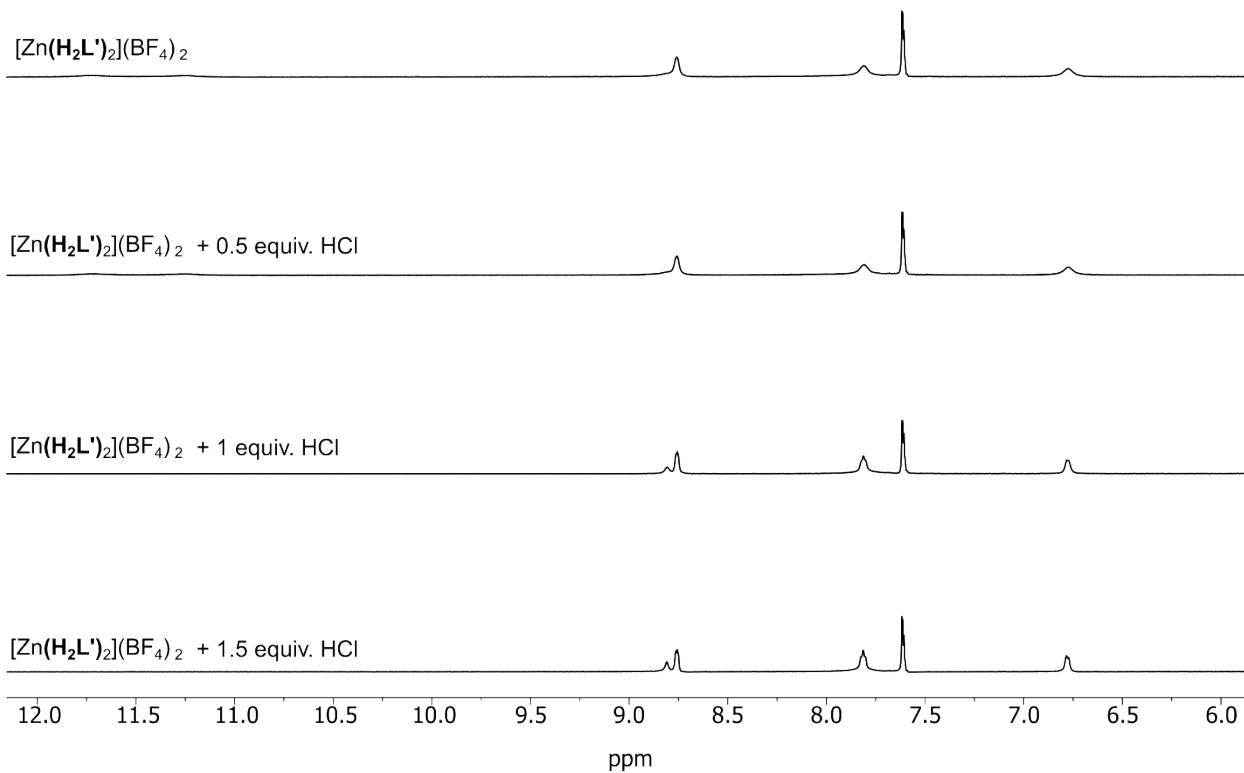
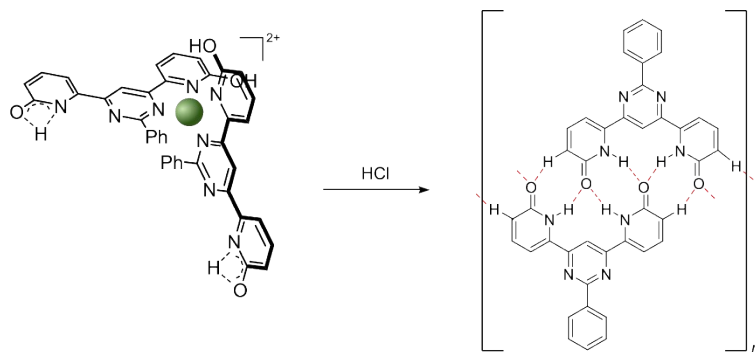


Figure S21. Titration of $[\text{Zn}(\text{H}_2\text{L}')_2](\text{BF}_4)_2$ with HCl (0.06 M, in $\text{DMSO-}d_6$) causing H_2L formation.

II. MOLECULAR MODELLING

The main goal of this ab-initio studies was to predict and depict the structures formed by ligand H_2L and its' iminol form $\text{H}_2\text{L}'$, including hydrogen-bonded aggregates and complex $[\text{Zn}(\text{H}_2\text{L}')_2](\text{BF}_4)_2$. A multi-step procedure was used to optimize the studied structures. The obtained structures were used as a blueprint for visualisation of polymeric species. All structures were pre-optimised with the semi-empirical RM1 method. The parameters for zinc atom were taken from the AM1 method. For H_2L , L^{2-} and $\text{H}_2\text{L}'$, the lowest-energy conformations were found using Gaussian's gmmx module. The input structures were then optimised with the DFT b3lyp/6-31+(g,d) method, which is a fair compromise between differing natures of the studied species and computational expenses, and ensures comparability of the results. To include dispersion effects, Grimme's D3 dispersion was added and complemented by Becke-Johnson (BJ) damping parameters for close-ranged interactions. Additional diffusion functions were included to correctly reproduce behaviour of anionic species. Polarization functions were added on hydrogen and the heavy atoms to reproduce correctly hydrogen. First, 2-pyridone and 2-pyridone dimer were optimized. The DFT functional PBE with base 6-31++G(d,p) was used and the calculation results obtained did reflect values reported in literature¹.

Table S1. The results of energy calculations of 2-pyridone molecule for monomeric and dimeric species. The H-Bond energy calculations were used for comparison to earlier reported values.

Base	2-pyridone [10^5 kcal mol ⁻¹]	2-pyridone dimer [10^5 kcal mol ⁻¹]	H-Bond [kcal mol ⁻¹]
pbepbe/6-311++g(d)	-2.0282	-4.0567	-20.55
ED3 correction	-	-4.0567	-6.78

Next was the optimisation of the H_2L structure itself. The H_2L molecule exists in amido-iminol tautomeric forms. The amido-form was found to be more stable (form C, Figure S1). Calculated single point energies for tautomers H_2L and $\text{H}_2\text{L}'$ show that H_2L has total energy lower by about 24.3 kJ/mol than $\text{H}_2\text{L}'$.

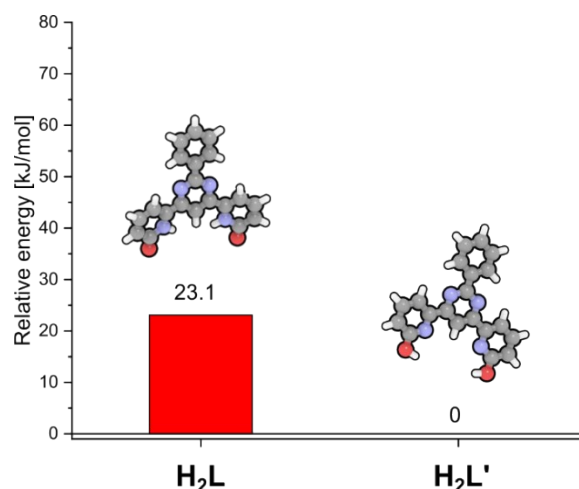
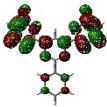
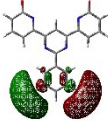



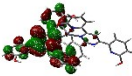

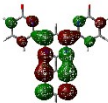


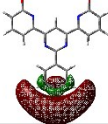
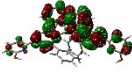
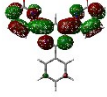
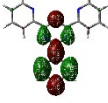

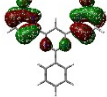
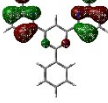
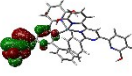
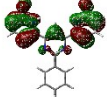
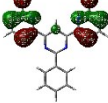
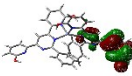
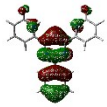
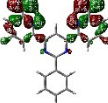
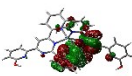
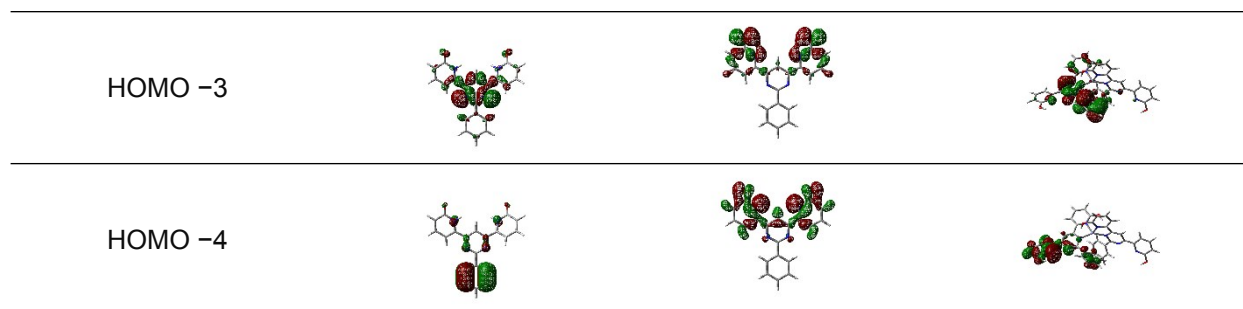


Figure S22. Relative energy of H_2L and $\text{H}_2\text{L}'$. The total energy of molecules was obtained using b3lyp/6-31+g(d,p) methodology and gd3bj dispersion and damping.

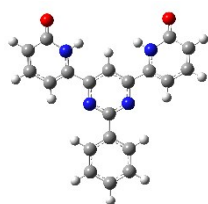
Intrinsic properties of a molecule can be predicted based on the distribution of energy levels of highest occupied molecular orbital (HOMO) and lowest unoccupied molecular orbital (LUMO). While the MO structure for both H_2L and H_2L' shows symmetrical pattern, the introduction of metal cation shows the shift of electronic cloud of bonding HOMO level towards the metal centre and shift of LUMO levels to the opposite side of molecule. For analysis 6-31g++(d,p) calculations for optimised structures of molecules were used.

Table S2. Frontier orbitals analysis.

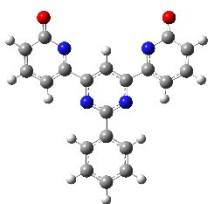
MO	H_2L	H_2L'	$[Zn(H_2L')_2](BF_4)_2$
LUMO +4			
LUMO +3			
LUMO +2			
LUMO +1			
LUMO			
HOMO			
HOMO -1			
HOMO -2			



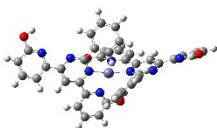
H₂L, L²⁻ anion and [Zn(H₂L')₂](BF₄)₂ structure description



H₂L: This structure can occur in several conformations, from of which the one shown, has the lowest energy. The pyridone rings are set relative to each other in a trans configuration, deflected relative to the plane of the central pyrimidine ring by about 21° in opposite directions. The phenyl ring is slightly displaced from the plane of the pyrimidine ring by a dihedral angle of 5.7 Å. The length of the C=O bonds in this molecule is 1.23 Å, while the N-C bonds of the amide group are 1.41 Å.



L²⁻ anion: The anionic form of iminol form of the structure was found to be flat. The length of the C-O bonds in this molecule is 1.26 Å, while the N-C bonds of the amide group are 1.39 Å.



[Zn(H₂L')₂](BF₄)₂: The structure of the complex consists of two ligand molecules in the iminol form, coordinated to the Zn²⁺ cation by the nitrogen atoms of the pyrimidine-pyridine pocket. The Zn-N bond lengths for pyridine nitrogen atoms are slightly longer than for pyrimidine nitrogen atoms, the average lengths of these bonds are 2.08 Å and 2.01 Å, respectively. The zinc cation is coordinated with the symmetry of a distorted tetrahedron. The dihedral angles between the pyridine and central ring are small for the coordinating unit, i.e. about 1-13°, while for phenyl rings, angles are on average 20.7°, which is similar to the free form **H₂L**. The dihedral angles between the phenyl ring and the pyrimidine ring have an average value of 36°. The bond lengths are as follows: C-O 1.34 Å, C-N 1.34 Å.

SambVca 2.1 steric hindrance results

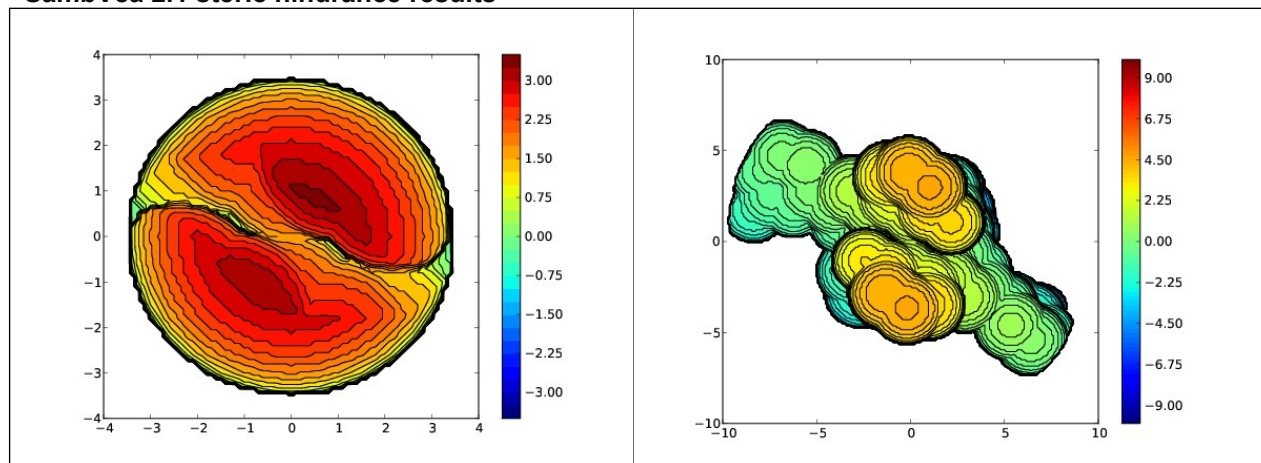


Figure S23. Steric maps calculated in SambVca software² for complex $[\text{Zn}(\text{H}_2\text{L}')_2](\text{BF}_4)_2$. Standard (3.5 Å) and enlarged (10 Å) radii were used.

Table S4. SambVca 2.1 steric hindrance results.

%V Free	%V Buried			
10.8	89.2			
Quadrant	V_{free}	V_{bur}	%V_{free}	%V_{bur}
SW	6	38.9	13.4	86.6
NW	5.8	39	13	87
NE	2.7	42.2	6	94
SE	4.8	40	10.8	89.2

III. SCANNING TUNNELING MICROSCOPY

General methods for STM experiments:

The solution was prepared by dissolving dyanmer H_2L or complex $[\text{Zn}(\text{H}_2\text{L}')_2](\text{BF}_4)_2$ in DMSO at slightly elevated temperatures (heat gun) and, additionally, in trichlorobenzene (TCB). For the measurements, a 20 μL drop of 5 μM of solution was casted onto the surface and heated up (using heating plate) to a temperature of 50-65 $^\circ\text{C}$ (determined empirically). The temperature was measured using a type K thermocouple spot-welded to the edge of the sample holder. The scanning was performed inside the solution drop, i.e. at the solid-liquid interface. The bias voltage was applied to the sample.

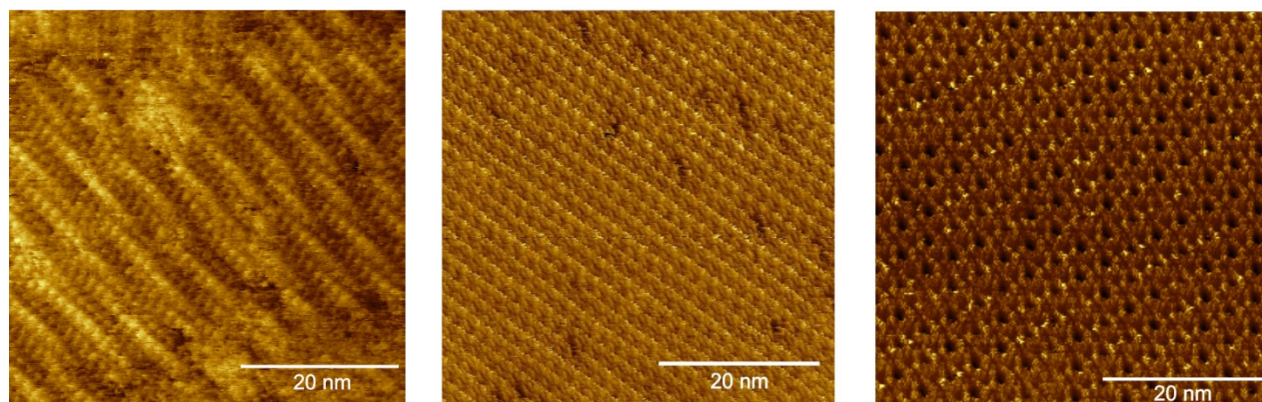


Figure S24. STM images of helical H_2L (left) H_2L 2D arrays (middle) and $[\text{Zn}(\text{H}_2\text{L}')_2](\text{BF}_4)_2$ (right). Images size: $50 \times 50 \text{ nm}^2$; $V_{\text{sample}} = +0.6 \text{ V}$; $I_T = 0.1 \text{ nA}$.

Both STM images of helical polymer H_2L (Fig. S24 left) and of 2D array of complex $[\text{Zn}(\text{H}_2\text{L}')_2](\text{BF}_4)_2$ (Fig. S24 right) were obtained from same sample by drop-casting $20 \mu\text{L}$ of $5 \mu\text{M}$ solution of $[\text{Zn}(\text{H}_2\text{L}')_2](\text{BF}_4)_2$ onto HOPG and heating to $50\text{--}65 \text{ }^\circ\text{C}$. This coexistence of both helical dynamers and 2D arrays made by complex $[\text{Zn}(\text{H}_2\text{L}')_2](\text{BF}_4)_2$ can be interpreted as confirmation of dynamic equilibrium between H_2L and $[\text{Zn}(\text{H}_2\text{L}')_2](\text{BF}_4)_2$. STM image of 2D array of H_2L (Fig. S24 middle) was obtained by drop-casting $20 \mu\text{L}$ of $5 \mu\text{M}$ of H_2L solution onto HOPG and heating to $50\text{--}65 \text{ }^\circ\text{C}$.

Using the methodology proposed by Gao et al^[3], for the given experimental conditions of the STM experiment, we compared the shape and the contours of the LUMO orbitals with the recorded STM images. The obtained structure match very well to the toroidal shapes in the STM image.

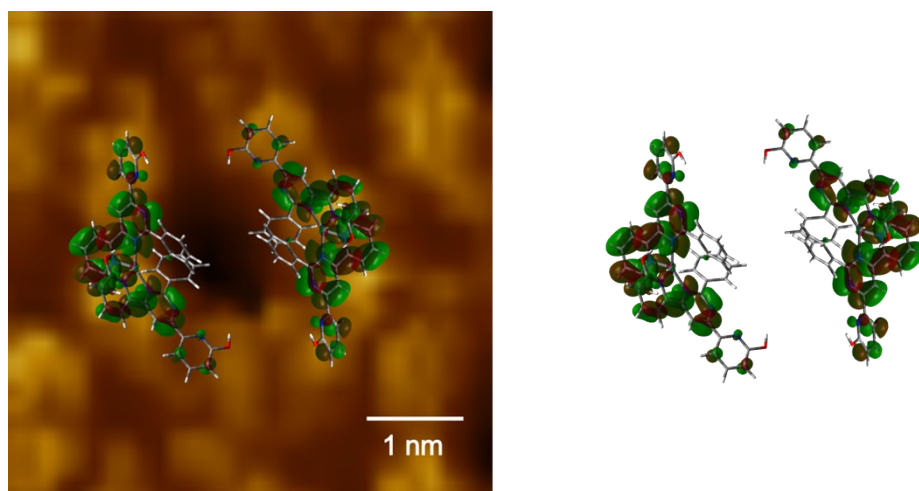


Figure S25. Zoomed area of STM image of $[\text{Zn}(\text{H}_2\text{L}')_2](\text{BF}_4)_2$ 2D arrays with model of LUMO orbitals of 2 molecules of $[\text{Zn}(\text{H}_2\text{L}')_2](\text{BF}_4)_2$ on top of it (left). Image size: $5 \times 5 \text{ nm}^2$; $V_{\text{sample}} = +0.6 \text{ V}$; $I_T = 0.1 \text{ nA}$. LUMO orbitals of 2 molecules of $[\text{Zn}(\text{H}_2\text{L}')_2](\text{BF}_4)_2$ (right).

References

- [1] Ciesielski, A., Stefankiewicz, A. R., Hanke, F., Persson, M., Lehn, J. M., & Samori, P. *Small* **2011**, *7*, 342–350.
- [2] Falivene, L. et al. *Nat. Chem.* **2019**, *11*, 872.
- [3] H. T. Zhou, J. H. Mao, G. Li, Y. L. Wang, X. L. Feng, S. X. Du, K. Müllen, H. J. Gao, *Applied Physics Letters* **2011**, *99*, 153101.